Taylor & Francis
Taylor & Francis Group

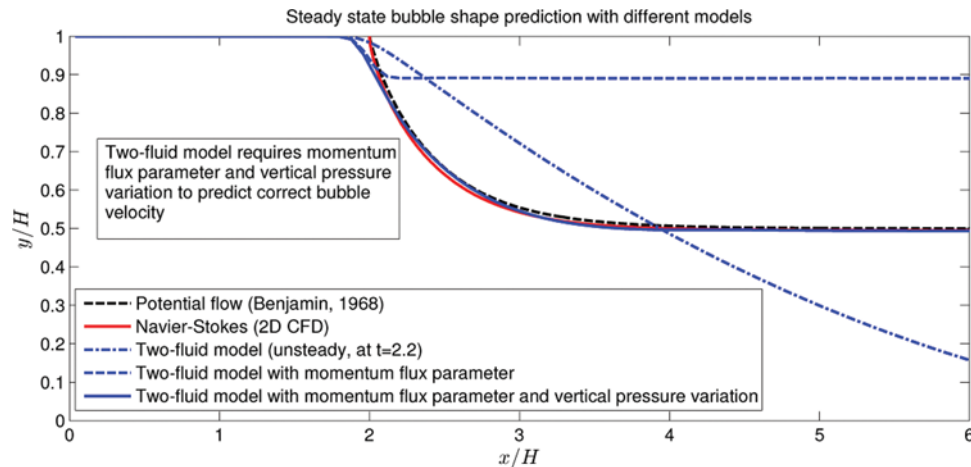# Simulation of Elongated Bubbles in a Channel Using the Two-Fluid Model

B. Sanderse,[1] M. Haspels,[1,2] and R. A. W. M. Henkes[1,3]

[1]*Shell Technology Centre Amsterdam, Amsterdam, The Netherlands*
[2]*Faculty of Engineering Technology, University of Twente, Enschede, The Netherlands*
[3]*Faculty 3ME, Delft University of Technology, Delft, The Netherlands*

GRAPHICAL ABSTRACT

This paper investigates the capability of the two-fluid model to predict the bubble drift velocity of elongated bubbles in channels. The two-fluid model is widely used in the oil and gas industry for dynamic multiphase pipeline simulations. The bubble drift velocity is an important quantity in predicting pipeline flushing and slug flow. In this paper, it is shown that the two-fluid model in its standard form predicts a bubble drift velocity of $\sqrt{gH}$ (similar to the shallow water equations), instead of the exact value of $\frac{1}{2}\sqrt{gH}$ as derived by Benjamin[1]. Modifying the two-fluid model with the commonly employed momentum correction parameter leads to a steady solution (in a moving reference frame), but still predicts an erroneous bubble drift velocity. To get the correct bubble drift velocity, it is necessary to include the pressure variation along the channel height due to both the hydrostatic component and the vertical momentum flux.

Keywords Elongated bubble, two-fluid model, Benjamin bubble, momentum flux parameter

1. INTRODUCTION

Accurate and efficient prediction of two-phase flow is essential for safe and cost-effective operation of pipelines in the oil and gas industry. An important case in pipeline operation is the flushing of a pipeline. For example, when a pipeline has been shut down for maintenance, it has to

Color versions of one or more of the figures in the article can be found online at www.tandfonline.com/ldis.

be pressure-tested before production can be continued. These pressure tests are conducted with water and the pipeline must be free of oil. The oil is removed out of the pipeline by flushing the pipeline with water. However, due to undulations in the terrain, segments of the pipeline may not be horizontal. Downward inclined segments, and especially v-sections, can then cause problems in the flushing process. This effect is shown schematically in Figure 1. If the water velocity is not sufficiently high, the oil will not be flushed out from the v-section of the pipeline, because the density of oil is lower than the density of water. To be precise, this happens when the water velocity is lower than the bubble drift velocity, which is the velocity that

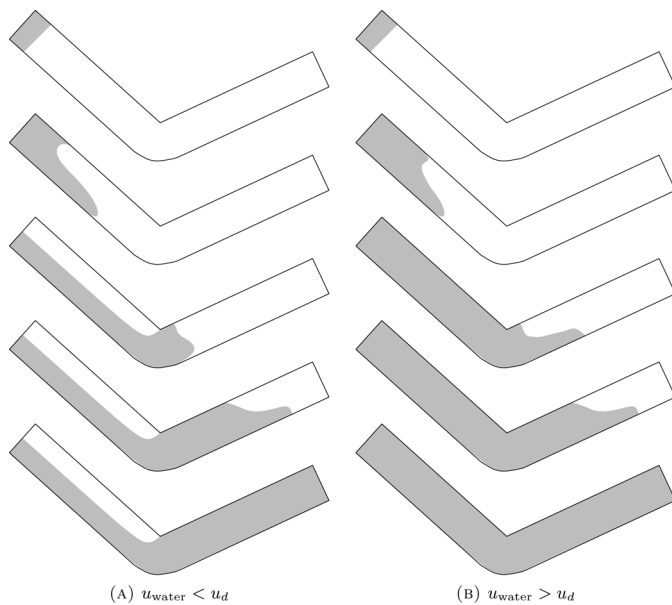(A) $u_{\text{water}} < u_d$ (B) $u_{\text{water}} > u_d$

FIG. 1. Transient behaviour of flushing a downward inclined pipeline depending on water velocity and bubble drift velocity.

an oil bubble has when it is moving into stagnant water. In this case, water can exit the pipeline without containing any oil, falsely indicating that all the oil is removed from the pipeline. On the other hand, when the water velocity is higher than the bubble drift velocity, all the oil will be flushed out of the pipeline. To determine the required water velocity to flush out all the oil from the pipeline, the bubble drift velocity of the oil must be predicted.

An elongated bubble rising in a stagnant liquid in a vertical pipe or channel is often referred to as a Dumitrescu or Taylor bubble. Dumitrescu[2] seems to be the first to derive an analytical solution for the bubble drift velocity and the bubble shape. For vertically rising bubbles reference is also made to the work of Taylor[3]. Benjamin[1] derived an analytical solution for the velocity of an elongated bubble that moves into a horizontal channel or pipe filled with a stagnant liquid, while neglecting viscosity and surface tension. The bubble drift velocity derived by Dumitrescu and Benjamin is, besides the application of pipeline flushing, an important quantity in the prediction of the bubble velocity in slug flows. Nicklin[4] proposed the following slug flow relation:

$$u_b = C_0 u_m + u_d, \qquad [1]$$

where u_b is the bubble velocity, u_m is the mixture velocity, u_d is the bubble drift velocity, and C_0 is a distribution parameter that has a value of about 2 for laminar flow. The Benjamin and Taylor bubble solutions are useful to obtain an estimate of the bubble drift velocity. However, in order to be used in a predictive model for multiphase

flow in an actual pipeline, more physical effects such as elevation changes, variations in density and phase split, viscosity and surface tension should be taken into account. It is therefore necessary to use more complete models. The most complete approach is to solve the three dimensional Navier–Stokes equations for both gas and liquid. The Benjamin and Taylor bubble solutions are particular solutions of these equations. However, solving the Navier–Stokes equations is computationally prohibitively expensive when long pipeline systems are considered. The Navier–Stokes equations are therefore simplified by employing averaging techniques that reduce the dimensionality of the problem. The one-dimensional two-fluid model[5,6] is the most commonly used model to simulate two-phase flow in pipelines or channels. However, the averaging process inevitably leads to a loss of information, which may require closure relations in the two-fluid model. An adaptation that has been suggested in literature is to use a so-called momentum flux parameter or momentum flux correction factor[7,8,9,10]. Andreussi et al.[11] report that corrections to the one-dimensional equations were necessary to obtain the bubble drift velocity, but do not provide details. It is therefore unclear yet if this parameter is sufficient to obtain the correct bubble drift velocity.

The central question in this paper is as follows: To what extent is the two-fluid model able to capture the bubble drift velocity given by the Benjamin bubble solution?

In order to answer this question we take the following approach. First, we use the results of two-dimensional Navier–Stokes computations to verify the shape of the Benjamin bubble (as derived in[1]). Second, we perform simulations with the two-fluid model in its basic form (i.e., without any closure relations) and show that for the case under consideration the solutions are equivalent to the shallow water equations. This will reveal that the bubble drift velocity predicted by the two-fluid model cannot be equal to the Benjamin bubble velocity. Third, we adapt the two-fluid model by introducing correction terms for the transport of momentum in both horizontal and vertical directions, which then leads to the correct bubble drift velocity. We have applied this analysis to inviscid flow in a horizontal channel, but the extension to inclined pipes is not too difficult.

The outline of the paper is as follows: In Section 2, we present the continuous models employed in this paper: Navier–Stokes, two-fluid model, shallow water and potential flow (Benjamin bubble). Then, in section 3, some details of the discretization of the two-fluid model and the Navier–Stokes equations are given. In section 4, the comparison between the different models is made, and the correction terms to the two-fluid model necessary to obtain the Benjamin bubble solution.

2. OVERVIEW OF CONTINUOUS MODELS

The Benjamin bubble appears when a pipe initially filled with liquid is opened at one side, so that a gas bubble penetrates into the liquid, and the liquid flows out of the opening. This is similar to the dam-break problem. In this paper, we will consider a reference frame attached to the bubble nose, and we look for steady solutions in this reference frame; this is a valid approach if viscosity (and thus the presence of a viscous boundary layer along the wall) can be neglected. A sketch of the problem is shown in Figure 2. An overview of the models considered in this study is given in Table 1.

2.1. Navier–Stokes Equations

The most complete model to describe the flow of bubbles in channels or pipelines is given by the Navier–Stokes equations. The compressible inviscid Navier–Stokes equations read, in integral form:

$$\frac{\mathrm{d}}{\mathrm{d}t}\int_\Omega \rho\mathrm{d}\Omega + \int_{\partial\Omega}\rho(\mathbf{u}-\mathbf{w})\cdot\mathbf{n}\mathrm{d}S = 0, \qquad [2]$$

$$\frac{\mathrm{d}}{\mathrm{d}t}\int_\Omega \rho\mathbf{u}\mathrm{d}\Omega + \int_{\partial\Omega}\rho\mathbf{u}(\mathbf{u}-\mathbf{w})\cdot\mathbf{n}\mathrm{d}S = -\int_{\partial\Omega}p\mathbf{n}\mathrm{d}S + \int_\Omega\rho\mathbf{g}\mathrm{d}\Omega, \qquad [3]$$

where $\mathbf{w}$ is the local velocity of the boundary. The integral form is chosen here because it is used to derive the two-fluid model in section 2.3. Equations (2) and (3) also hold in multiphase flow, provided that near interfaces the correct jump conditions are taken into account. For the inviscid case under consideration, the interface conditions are continuity of mass flux (no phase transition), and continuity of pressure (no surface tension).

2.2. Potential Flow

If the flow can be assumed inviscid, irrotational, and incompressible, the conservation of mass equation can be written in terms of the velocity potential ϕ ($\mathbf{u}=\nabla\phi$),

$$\nabla^2\phi = 0. \qquad [4]$$

At the same time, the momentum equations simplify to the Bernoulli relation

$$p+\frac{1}{2}\rho(u^2+v^2)+\rho g y = \text{constant} \quad \text{along a streamline.} \quad [5]$$

Benjamin[1] used these relations to derive the following relations for the downstream velocity and liquid height in a channel:

$$u_{\mathrm{in}} = \frac{1}{2}\sqrt{gH}, \qquad [6]$$

$$u_{\mathrm{out}} = \sqrt{gH} \qquad [7]$$

$$h_{\mathrm{out}} = \frac{1}{2}H, \qquad [8]$$

and an approximate solution for the bubble shape, which will not be repeated here.

2.3. Two-Fluid Model

The two-fluid model can be derived by applying the integral form of the Navier–Stokes equations (2) and (3), to a gas or liquid phase occupying part of a channel segment. We consider a channel aligned with the x-axis, and consider the control volume for the liquid as depicted in Figure 3. The interface moves with a velocity $\mathbf{w}$.

Assuming that the variation of density across the height of the channel is negligible, and assuming that there is no mass transfer across the interface (so $\mathbf{u}\cdot\mathbf{n}=\mathbf{w}\cdot\mathbf{n}$ on the interface), conservation of mass for this control volume reads

$$\frac{\mathrm{d}}{\mathrm{d}t}\int_x^{x+\Delta x}\rho h(x^*)\mathrm{d}x^* + \rho h(x+\Delta x)\bar{u}(x+\Delta x) - \rho h(x)\bar{u}(x) = 0, \qquad [9]$$

where the average velocity over the height h is defined as

$$\bar{u}(x) = \frac{1}{h(x)}\int_0^{h(x)}u(x,y)\mathrm{d}y. \qquad [10]$$

In the limit of $\Delta x\to 0$, this can be written as

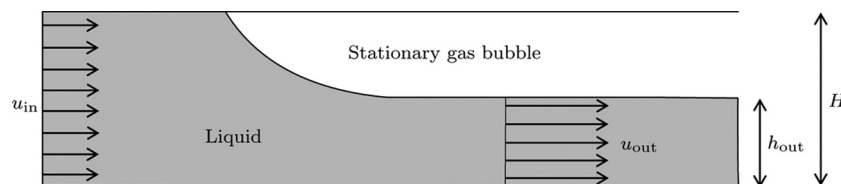$$\frac{\partial}{\partial t}(\rho h(x)) + \frac{\partial}{\partial x}(\rho\bar{u}(x)h(x)) = 0. \qquad [11]$$

FIG. 2. Benjamin bubble in a reference frame attached to the bubble nose.

TABLE 1
Classification of models

	1D	2D
Analytical solution	Shallow water equations	Potential flow
Approximate solution	Two-fluid model	Navier–Stokes

Within the assumption of negligible density variation in y-direction, this relation is still exact, that is, no assumptions regarding the one-dimensional nature of the velocity field have been made.

In a similar fashion one can derive the height-averaged u- and v-momentum equations. Taking the inner product of Equation (3) with $\mathbf{e}_x$ gives

$$\frac{\mathrm{d}}{\mathrm{d}t}\int_\Omega \rho u\,\mathrm{d}\Omega + \int_{\partial\Omega}\rho u(\mathbf{u}-\mathbf{w})\cdot\mathbf{n}\mathrm{d}S = -\int_{\partial\Omega}pn_x\mathrm{d}S. \quad [12]$$

When evaluated for the control volume in Figure 3 this becomes

$$\frac{\mathrm{d}}{\mathrm{d}t}\int_x^{x+\Delta x}\rho h(x^*)\overline{u}(x^*)dx^* + \rho h(x+\Delta x)\overline{u^2}(x+\Delta x)$$
$$- \rho h(x)\overline{u^2}(x) =$$
$$-\left(h(x+\Delta x)\overline{p}(x+\Delta x) - h(x)\overline{p}(x) - \int_{h(x)}^{h(x+\Delta x)}p_{\mathrm{int}}(x)\mathrm{d}h\right). $$
$$[13]$$

In the limit of $\Delta x \to 0$ this reduces to

$$\frac{\partial}{\partial t}(\rho h(x)\overline{u}(x)) + \frac{\partial}{\partial x}(\rho h(x)\overline{u^2}(x)) = -\frac{\partial}{\partial x}(h(x)\overline{p}(x))$$
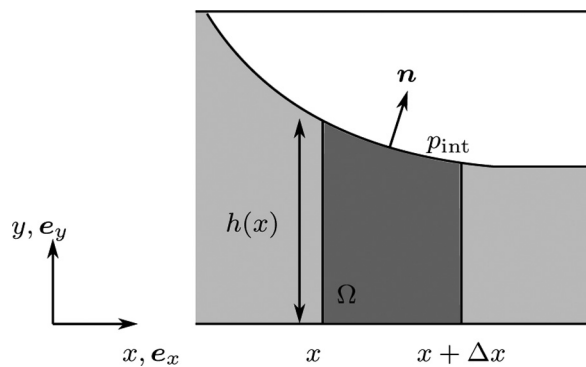$$+ p_{\mathrm{int}}(x)\frac{\partial h(x)}{\partial x}. \quad [14]$$

FIG. 3.   Control volume for deriving the two-fluid model equations.

The same procedure can be applied to the v-momentum equation. Taking the inner product of Equation (3) with $\mathbf{e}_y$ gives

$$\frac{\mathrm{d}}{\mathrm{d}t}\int_\Omega \rho v\mathrm{d}\Omega + \int_{\partial\Omega}\rho v(\mathbf{u}-\mathbf{w})\cdot\mathbf{n}\,\mathrm{d}S = -\int_{\partial\Omega}pn_y\,\mathrm{d}S - \int_\Omega \rho g\,\mathrm{d}\Omega.$$
$$[15]$$

When applied on a control volume, it reads

$$\frac{\mathrm{d}}{\mathrm{d}t}\int_x^{x+\Delta x}\rho h(x^*)\overline{v}(x^*)\mathrm{d}x^* + \rho h(x+\Delta x)\overline{uv}(x+\Delta x)$$
$$- \rho h(x)\overline{uv}(x) = -\int_x^{x+\Delta x}(p_{\mathrm{int}}(x^*) - p(x,y=0))\mathrm{d}x^* \quad [16]$$
$$- \int_x^{x+\Delta x}\rho gh(x^*)\mathrm{d}x^*,$$

which in the limit of $\Delta x \to 0$ becomes

$$\frac{\partial}{\partial t}(\rho h\overline{v}) + \frac{\partial}{\partial x}(\rho h\overline{uv}) = -(p_{\mathrm{int}} - p(x^*,y=0)) - \rho gh, \quad [17]$$

where we dropped the explicit dependency on (x). Again, Equations (11), (14), and (17) are still exact, and *the Benjamin bubble solution thus is a valid solution to Equations* (11), (14), *and* (17).

However, the averaging process inevitably leads to a loss of information; the system of equations features more unknowns than equations. In order to derive a closed system of one-dimensional equations in terms of $\bar{u}(x)$, $p_{\mathrm{int}}(x)$, and $h(x)$, a number of assumptions have to be made. The main assumption that leads to the two-fluid model is that the flow is one-dimensional, which implies that:

- the average of products can be approximated by the product of averages:

$$\overline{u^2} \approx \overline{u}^2, \quad [18]$$

- the vertical velocity $v \approx 0$, and the pressure thus varies hydrostatically in vertical direction:

$$p(x,y) = p_{\mathrm{int}}(x) - \rho g(y - h(x)). \quad [19]$$

From the last equation, one can derive the relation between the average pressure and the interface pressure:

$$h(x)\overline{p}(x) = \int_0^{h(x)}p(x,y)\mathrm{d}y = \int_0^{h(x)}(p_{\mathrm{int}}(x) - \rho g(y - h(x)))\mathrm{d}y$$
$$= h(x)p_{\mathrm{int}}(x) + \tfrac{1}{2}\rho gh(x)^2.$$
$$[20]$$

Substituting Equations (18) and (20) into (14) and (17) then gives the conservation equations for the liquid phase. Applying the same technique to the gas phase leads to the

inviscid, compressible two-fluid model equations:

$$\frac{\partial}{\partial t}(\rho_l h_l) + \frac{\partial}{\partial x}(\rho_l \overline{u_l} h_l) = 0, \qquad [21]$$

$$\frac{\partial}{\partial t}(\rho_g h_g) + \frac{\partial}{\partial x}(\rho_g \overline{u_g} h_g) = 0, \qquad [22]$$

$$\frac{\partial}{\partial t}(\rho_l h_l \overline{u_l}) + \frac{\partial}{\partial x}(\rho_l h_l \overline{u_l}^2) = -h_l \frac{\partial p_{int}}{\partial x} - \frac{\partial}{\partial x}\left(\frac{1}{2}\rho_l g h_l^2\right), \quad [23]$$

$$\frac{\partial}{\partial t}(\rho_g h_g \overline{u_g}) + \frac{\partial}{\partial x}(\rho_g h_g \overline{u_g}^2) = -h_g \frac{\partial p_{int}}{\partial x} - \frac{\partial}{\partial x}\left(\frac{1}{2}\rho_g g h_g^2\right), \qquad [24]$$

supplemented with the constraint that the two phases together occupy the channel:

$$h_g + h_l = H. \qquad [25]$$

The coupling between the gas phase and the liquid phase occurs via the interface pressure p_{int}. The system of equations is well-posed and stable as long as the velocity difference between the phases does not exceed the inviscid Kelvin–Helmholtz limit. It is, however, unclear if the Benjamin bubble solution is also a solution to the two-fluid model Equations (21)–(24). This will be further explored in section 2.5.

2.4. Shallow Water Equations

The coupling between the gas and liquid phase is negligible, as is the case in the Benjamin bubble solution (which has been obtained for a negligibly small gas density), the two-fluid model can be further simplified. After assuming $\frac{\partial p_{int}}{\partial x} = 0$ and assuming incompressible flow, the shallow water equations for the liquid phase are obtained:

$$\frac{\partial}{\partial t}(h_l) + \frac{\partial}{\partial x}(h_l \overline{u_l}) = 0, \qquad [26]$$

$$\frac{\partial}{\partial t}(h_l \overline{u_l}) + \frac{\partial}{\partial x}\left(h_l \overline{u_l}^2 + \frac{1}{2}g h_l^2\right) = 0. \qquad [27]$$

This system of equations is in conservative form. The eigenvalues of the system are

$$\lambda_{1,2} = \overline{u_l} \pm \sqrt{g h_l}. \qquad [28]$$

Compared to the two-fluid model, two eigenvalues related to the compressibility of the liquid and gas (speed of sound) have disappeared. Since the assumptions made in the shallow water equation derivation are correct for the case of the Benjamin bubble (negligible interface pressure, incompressible liquid), we expect that for the Benjamin bubble case the eigenvalues of the two-fluid model will be very

close to the eigenvalues of the shallow water equations (except for the two additional eigenvalues that are related to the speed of sound of the gas phase).

In case of the dam-break problem with a dry ground on one side, like the initial condition of the Benjamin bubble solution, an analytical solution to the shallow water equations exists. That solution consists of an expansion wave whose head is moving with speed $2\sqrt{g h_l}$ and whose tail is moving with speed $-\sqrt{g h_l}$ (in a fixed reference frame). The analytical solution for $-\sqrt{g h_l}t < x < 2\sqrt{g h_l}t$ is[12]

$$h(x,t) = \frac{h_l}{9}\left(2 - \frac{x}{\sqrt{g h_l}t}\right)^2, \qquad [29]$$

and

$$u(x,t) = \frac{2}{3}\left(\frac{x}{t} + \sqrt{g h_l}\right). \qquad [30]$$

h and hu are continuous throughout the domain, but u jumps at $x = 2\sqrt{g h_l}t$.

2.5. Corrected Two-Fluid Model

We will now show that the two-fluid model Equations (21)–(24) cannot predict the Benjamin bubble as obtained by potential flow theory (section 2.2). Consider the part of the solution that is single phase ($h_l = H$). In steady state, conservation of mass and momentum of the incompressible liquid phase read

$$\frac{\partial}{\partial x}(H\overline{u_l}) = 0, \qquad [31]$$

$$\frac{\partial}{\partial x}(\rho_l H \overline{u_l}^2) = -H\frac{\partial p_{int}}{\partial x}, \qquad [32]$$

where p_{int} is now to be interpreted as the pressure at the top of the channel. These equations reduce to

$$\frac{\partial p_{int}}{\partial x} = 0. \qquad [33]$$

Obviously, this is in conflict with the Benjamin bubble solution, where the pressure increases along the top of the channel until the bubble stagnation point is reached: *the two-fluid model cannot capture the Benjamin bubble.*

To identify the cause of the problem, we return to Equation (14), which is simply an integral version of the Navier–Stokes equations, and compare it with the two-fluid model equations. It is instructive to rewrite equation (14) in the form of Equation (23) but with additional correction terms that account for the assumptions made in the two-fluid model:

$$\frac{\partial}{\partial t}(\rho_l h_l \overline{u}) + \frac{\partial}{\partial x}(\rho_l h_l \beta \overline{u_l}^2) = -\frac{\partial}{\partial x}(h_l(\overline{p} - p_{int})) - h_l\frac{\partial p_{int}}{\partial x}, \qquad [34]$$

where

$$\beta = \frac{\overline{u_l^2}}{\overline{u_l}^2} \qquad [35]$$

is the momentum flux parameter or momentum correction factor[8,7]. For steady laminar single-phase flow (Poiseuille flow), β can be computed and equals $\frac{6}{5}$. The presence of β and the fact that we did not assume a hydrostatic balance of the form (19) to evaluate $\bar{p} - p_{\text{int}}$ keeps Equation (34) exact.

In general, Equation (17) cannot be easily cast into an explicit expression for $\bar{p} - p_{\text{int}}$. Fortunately, in the case of the steady Benjamin bubble the momentum equations can be integrated along a streamline giving the Bernoulli relation (5). Tracing back the streamlines to a reference point far upstream, the pressure at any point in the flow can be written as

$$p(x, y) = p_{\text{ref}} + \frac{1}{2}\rho(u_{\text{ref}}^2 - u^2 - v^2) + \rho g(y_{\text{ref}} - y). \qquad [36]$$

The reference point y_{ref} follows from conservation of mass:

$$u_{\text{ref}} y_{\text{ref}} = \int_0^y u(x, y^*) dy^*. \qquad [37]$$

The average pressure for the Benjamin bubble is then

$$\bar{p} = p_{\text{ref}} + \frac{1}{2}\rho u_{\text{ref}}^2 - \frac{1}{2}\rho(\overline{u^2} + \overline{v^2}) +$$
$$\rho g \int_0^{h(x)} \int_0^y \frac{u(x, y^*)}{u_{\text{ref}}} dy^* dy - \frac{1}{2}\rho g h^2. \qquad [38]$$

3. OVERVIEW OF DISCRETE MODELS

3.1. Solution of the Navier–Stokes Equations with Fluent

The solution of the Navier–Stokes equations (2) and (3) has been obtained by using the commercial computational fluid dynamics (CFD) software Fluent (ANSYS 14.0), which utilizes the finite-volume method (FVM). In order to be able to simulate multiphase flow, the volume of fluid (VOF) method has been employed. The inflow is adapted such that the position of the bubble nose remains fixed. For more details we refer to Kroes and Henkes[13].

3.2. Discretization of the Two-Fluid Model

The two-fluid model, Equations (21)–(25), are discretized in space by using a FVM on a staggered grid. The convective terms in both the mass and momentum equations are interpolated with a high-resolution scheme using the van Albada limiter. This is necessary to capture the shock and expansion waves that can be present in the two-fluid model. All other terms are approximated by central differences. The discretization in time is done with the second-order backward differentiation formula (BDF2) method; the resulting nonlinear system is solved using Newton's method. For more details, we refer to Appendix.

At the left boundary of the computational domain, the mass flow is prescribed. At the right boundary, the pressure is prescribed.

3.2.1. Single-Phase Flow Treatment

In regions where one of the phases is absent, the momentum equation corresponding to the absent phase is not solved since there exists no unique solution for the velocity of the absent phase. When a phase is almost vanishing, special care has to be taken, because the Jacobians in Equation (67) can become close to singular. Hence, the phase mass and velocity are set to zero when the phase height drops below a threshold value. The mass corresponding to the height beneath this threshold value is transported to the surrounding volumes using sink and source terms.

4. RESULTS

In this section, we take the following approach to identify which terms are necessary to make the two-fluid model suitable for simulating elongated bubbles. First, we check the Benjamin bubble solution with the 2D inviscid CFD solution obtained with Fluent. Second, we compare the solution of the two-fluid model with the solution of the shallow water equations and check the propagation (bubble) speed in both models. Finally, we use the corrected two-fluid model to simulate the Benjamin bubble.

Note that in presenting the results we use the following dimensionless quantities:

$$x^* = x/H, \quad y^* = y/H, \quad h^* = h/H, \qquad [39]$$

$$u_g^* = u_g/\sqrt{gH}, \quad u_l^* = u_l/\sqrt{gH}, \qquad [40]$$

$$p^* = (p - p_0)/\rho_l gH, \qquad [41]$$

$$t^* = t/\sqrt{H/g}. \qquad [42]$$

4.1. Validation of Benjamin Bubble Solution with 2D Inviscid CFD Solution

In Figure 4, we show the comparison between the 2D CFD results and the Benjamin bubble solution. The 2D CFD results have been computed on a 1600×200 mesh. There is a small difference between the two solutions that is mainly due to the smoothness of the interface representation in the VOF method, and the constant pressure boundary condition at $x^* = 8$. These differences disappear upon refining the mesh and extending the domain. There is
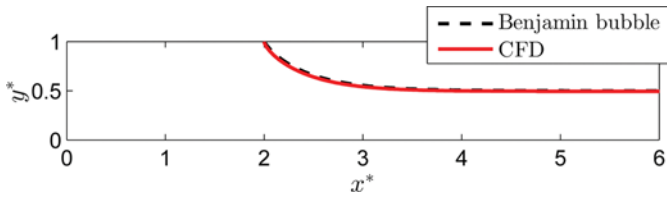
FIG. 4. Solution of dam-break problem with CFD and comparison with Benjamin bubble solution.

a very good agreement between the approximate solution for the bubble shape as derived by Benjamin and the CFD simulations, which means that the Benjamin bubble results can indeed be used as a reference for improving the two-fluid model.

Using the bubble shape as predicted in the Benjamin bubble solution, it is straightforward to obtain the velocity and pressure field in the liquid. First, the streamfunction ψ is computed by solving the Laplace equation

$$\nabla^2\psi = 0, \qquad [43]$$

with a finite difference method and Dirichlet boundary conditions on all sides (note that the bubble itself is a streamline of the flow). The velocity follows as $\mathbf{u} = \nabla \times \boldsymbol{\Psi}$ ($\boldsymbol{\Psi} = \Psi\mathbf{e}_z$), and the pressure from Equation (36). The resulting streamfunction, velocity, and pressure field are shown in Figure 5; the streamfunction and velocity have been non-dimensionalized with $\sqrt{gH}$ (note that the pressure shown does not include the gravitational contribution). As expected, the CFD results obtained with Fluent are very
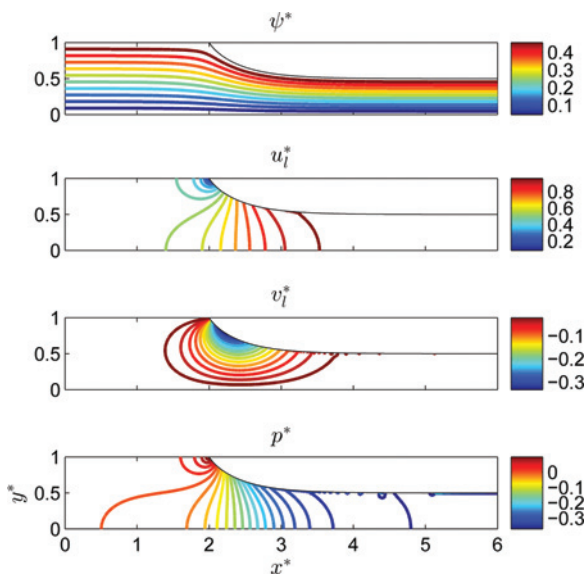
similar. Small disturbances near the interface can be seen in the vertical velocity and pressure contours, which are due to numerical differentiation of the streamfunction. They disappear upon grid refinement. Figure 5 reveals that the horizontal velocity u has a significant two-dimensional nature, and that the vertical velocity component is clearly nonzero near the bubble nose.

4.2. Validation of Two-Fluid Model with Shallow Water Equations

As a next step, we compute the bubble velocity of the standard, unadjusted, two-fluid model. We simulate the dam-break problem as described in section 4.1. The discretization features 200 points in axial direction, and the simulation is marched with a (dimensionless) time step of 0.0125 to an end time of 2.2 (the CFL number based on the maximum liquid velocity is approximately 0.5). In Figure 6, the solution of the two-fluid model, for the liquid height and liquid velocity, is compared to the analytical solution to the dam-break problem, using the shallow water Equations (29) and (30). The two-fluid model also provides the gas velocity and the pressure, which are not part of the shallow water equations. The small pressure deviations are the effect of the compressibility of the gas phase. The shape of the curve for the gas velocity could have been expected based on the fact that the flow is almost

FIG. 5. Benjamin bubble solution in terms of streamfunction, horizontal and vertical velocity, and pressure.
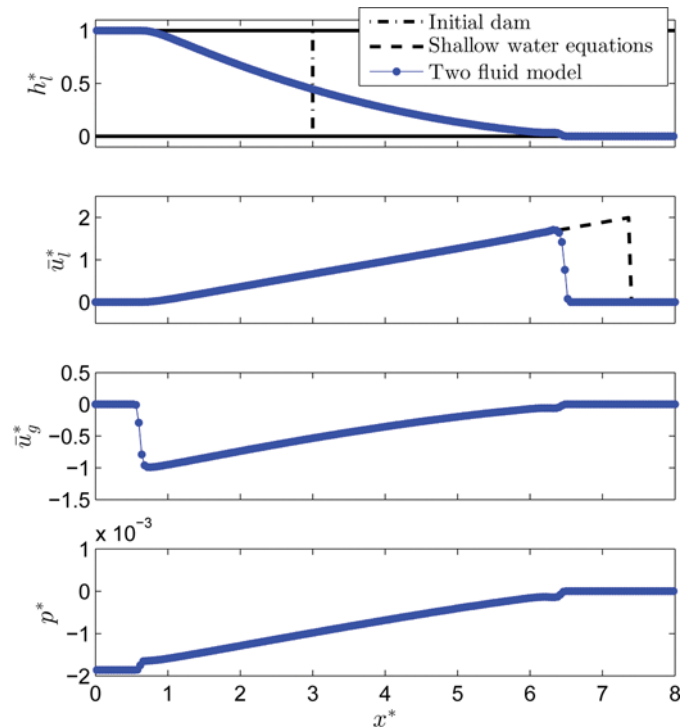

FIG. 6. Unsteady solution of dam-break problem with the standard two-fluid model and the shallow water equations. Gas velocity and pressure only available in two-fluid model solution.

incompressible, which implies that the mixture velocity $h_l^* u_l + h_g^* u_g$ is constant. It can be seen that, due to the very small pressure deviation, the two-fluid model results are essentially equivalent to the shallow water equations. This is due to the large density ratio between the liquid and the gas. The difference in liquid velocity at the tail of the bubble is a discretization effect that disappears upon grid refinement. The seemingly large difference is due to the fact that the liquid momentum is divided by the small liquid height value; the liquid momentum is more accurately captured than the liquid velocity.

The bubble nose moves with a velocity $-\sqrt{gH}$ and the tail with a velocity $2\sqrt{gH}$. This means that, in contrast to the Benjamin bubble solution, in a reference frame moving with the nose velocity $\sqrt{gH}$, the tail of the bubble will keep on moving to the right with speed $3\sqrt{gH}$. When time passes on, the region behind the nose will be filled with liquid—there is no steady state solution.

To summarize, this dam-break test case confirms that the bubble drift velocity of the two-fluid model is $\sqrt{gH}$ instead of $\frac{1}{2}\sqrt{gH}$, which is predicted by the Benjamin bubble solution, and that the two-fluid model does not possess a steady state solution in a reference frame attached to the bubble.

4.3. Simulating the Benjamin Bubble with the Corrected Two-Fluid Model

It is clear from section (4.2) that the two-fluid model gives the wrong bubble drift velocity. In this section, we investigate the effect of β and the additional effect of the nonzero vertical velocity component on the pressure.

4.3.1. Including β

When including the momentum correction factor β, the momentum equation that is solved for the liquid is:

$$\frac{\partial}{\partial t}\left(\rho_l h_l \overline{u}\right) + \frac{\partial}{\partial x}\left(\rho_l h_l \beta \overline{u_l}^2\right) = -h_l \frac{\partial p_{\text{int}}}{\partial x} - \frac{\partial}{\partial x}\left(\frac{1}{2}\rho_l g h_l^2\right).$$

[44]

β is shown in Figure 7 and is determined from the Benjamin bubble solution by integrating the velocity
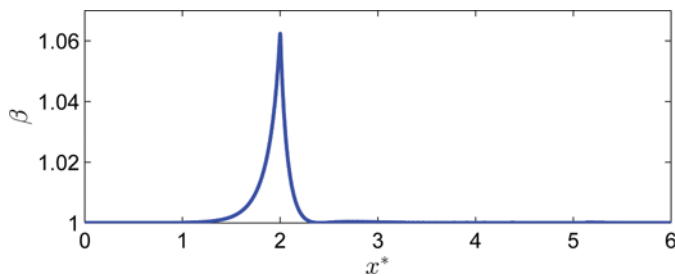

FIG. 7. β determined from Benjamin bubble solution.

profiles. β for the bubble in the channel is lower than the value of $\frac{4}{3}$ found for Poiseuille flow in a channel, and it is in fact close to 1 except for a small region close to the bubble nose where it is somewhat larger than 1. The results for the dam-break problem are shown in Figure 8. In contrast to Figure 6, where no steady state solution exists, the effect of β is that a steady state solution can be obtained: the liquid velocity and height reach constant values downstream of the bubble nose. However, *the bubble drift velocity is not correctly predicted:* $\sqrt{gH}$ instead of $\frac{1}{2}\sqrt{gH}$. This is because the smallest eigenvalue of the two-fluid model adapted with β is the same as for the shallow water equations when the liquid phase is stagnant: $-\sqrt{gH}$. Consequently, the liquid height downstream of the bubble is also not correct. Furthermore, the pressure change in front of the bubble nose displays incorrect behavior. When considering the steady state momentum and mass equations in the single-phase liquid region, we find that

$$\frac{\partial p_{\text{int}}}{\partial x} = -\rho_l \overline{u_l}^2 \frac{\partial \beta}{\partial x}.$$

[45]

Since in the single phase region $\overline{u_l}$ is constant and $\partial \beta / \partial x > 0$, this equation reveals that the pressure *drops* in the region in front of the bubble nose, as can be observed in the lowest plot in Figure 7. However, this is different
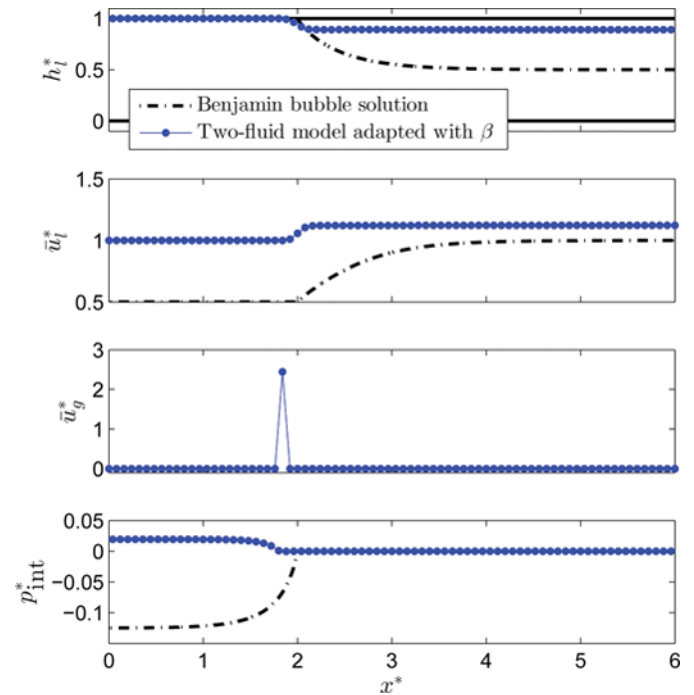

FIG. 8. Steady-state solution of dam-break problem with the two-fluid model adapted with β.

from the result for the Benjamin bubble, as found by applying the Bernoulli equation to the upper streamline:

$$\frac{\partial p_{\text{int}}}{\partial x} = -\rho_l u_l \frac{\partial u_l}{\partial x}. \qquad [46]$$

This predicts a pressure *increase* due to a velocity decrease toward the stagnation point. From the stagnation point to a point far downstream, the interface pressure is approximately constant, like in the Benjamin bubble and shallow water solutions. The liquid momentum balance between the bubble nose and a point far downstream thus reads:

$$\left[\rho_l h_l \beta \overline{u_l}^2 + \frac{1}{2} \rho_l g h_l^2 \right]_{\text{out}} - \left[\rho_l h_l \beta \overline{u_l}^2 + \frac{1}{2} \rho_l g h_l^2 \right]_{\text{nose}} = 0. \qquad [47]$$

After assuming that the flow in front of the bubble nose is single phase (and employing conservation of mass), this equation can be rewritten as

$$\left(\frac{\overline{u}_{\text{out}}}{\overline{u}_{\text{in}}} \right)^3 - \left(\beta_{\text{nose}} + \frac{\frac{1}{2} gH}{\overline{u}_{\text{in}}^2} \right) \left(\frac{\overline{u}_{\text{out}}}{\overline{u}_{\text{in}}} \right)^2 + \frac{\frac{1}{2} gH}{\overline{u}_{\text{in}}^2} = 0. \qquad [48]$$

This is a cubic equation in $\overline{u}_{\text{out}}$, for which an exact solution can be obtained with Cardano's formula; the result is shown in Figure 9. The striking conclusion from Equation (48) is that *the downstream velocity and height only depend on β at the bubble nose.* The shape of β in front and behind the bubble nose is not affecting the outlet velocity, as long as the liquid in front of the bubble nose is single phase, and as long as $\beta = 1$ far upstream and far downstream of the bubble. For the Benjamin bubble solution, $\beta_{\text{nose}} \approx 1.063$, and the expected dimensionless downstream velocity is $u_{\text{out}}^* \approx 1.24$. The numerically calculated value (see Figure 8) is approximately 1.12 when using 100 grid points. This discrepancy is due to the fact that the bubble nose position in the numerical solution is somewhat shifted forward due to discretization errors, leading to an effective β_{nose} that is lower than 1.063. Another discrepancy in the numerical
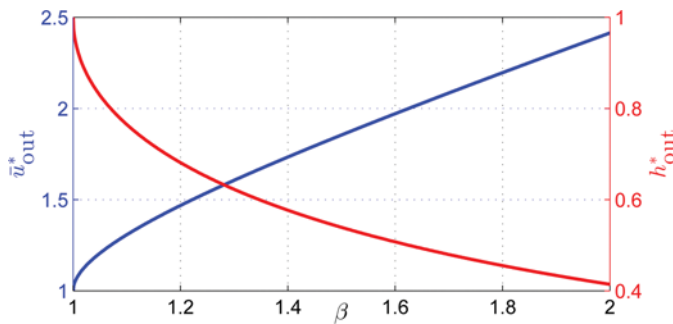
solution is that there is a peak in the gas velocity just upstream of the bubble nose; similar to section 4.2, this is related to the division of small gas momentum by small gas height.

The error in the bubble drift velocity is due to the assumption of hydrostatic pressure variation. This can be seen more clearly by comparing the level gradient term

$$\frac{\partial}{\partial x} \left(\frac{1}{2} \rho_l g h_l^2 \right), \qquad [49]$$

to the exact integrated pressure variation

$$\frac{\partial}{\partial x} (h(\overline{p} - p_{\text{int}})). \qquad [50]$$

Both terms are displayed in Figure 10. Although the area under the curve is the same for both (as follows from global momentum conservation), they have quite different characteristics. The level gradient term, as used in this section, does not reveal the change in pressure gradient in front of the bubble nose, because the flow is single phase in this region. The exact integrated pressure gradient, however, shows a clear decrease in front of the bubble nose, responsible for the deceleration of the flow. The interface pressure increases gradually near the bubble nose, and then changes its slope along the bubble interface. This causes the discontinuity in the integrated pressure gradient. In the next section, we will show that incorporating the exact integrated pressure term indeed leads to the correct bubble velocity.

4.3.2. Including β and Vertical Momentum Flux

Although including β leads to a steady solution, and a pressure effect upstream of the bubble, the bubble drift velocity is not yet correctly predicted. In this section, we also include the effect of the vertical momentum flux on
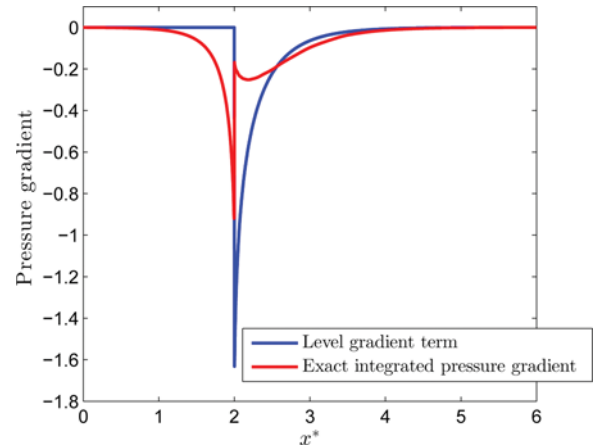

FIG. 9. Analytical outlet velocity and outlet height as function of β as given by equation (48).

FIG. 10. Comparison of level gradient term $\frac{\partial}{\partial x} \left(\frac{1}{2} \rho_l g h_l^2 \right)$ and exact pressure variation $\frac{\partial}{\partial x} (h(\overline{p} - p_{\text{int}}))$.
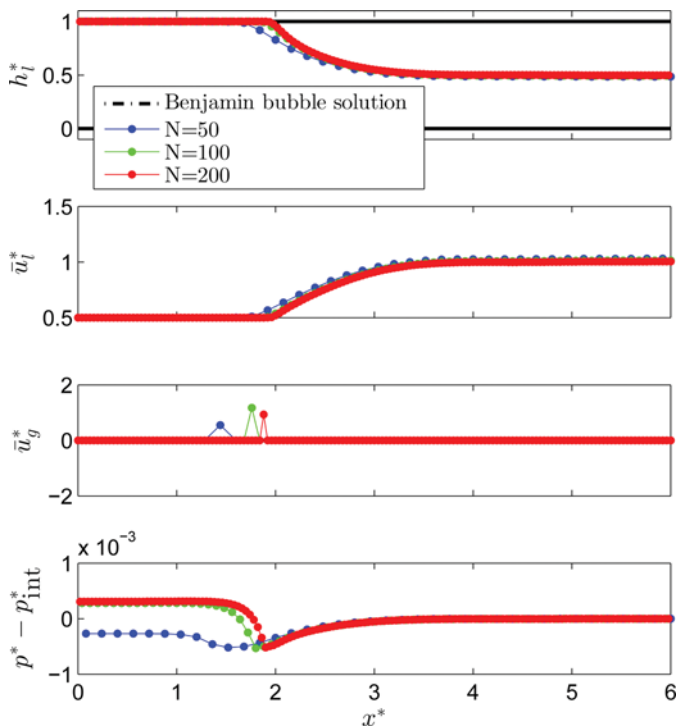
FIG. 11. Steady-state solution of dam-break problem with the two-fluid model adapted with β and vertical momentum flux.

the height-averaged pressure term, that is, we solve

$$\frac{\partial}{\partial t}\left(\rho_l h_l \overline{u}\right) + \frac{\partial}{\partial x}\left(\rho_l h_l \beta \overline{u_l}^2\right) = -\frac{\partial}{\partial x}\left(h_l(\overline{p} - p_{\text{int}})\right) - h_l\frac{\partial p_{\text{int}}}{\partial x},$$
[51]

with $\overline{p}$ given by (38). The results for this model are shown in Figure 11. It can be seen that the additional effect of the vertical momentum flux on the channel-averaged pressure is to obtain the correct Benjamin bubble solution: the drift velocity is $\frac{1}{2}\sqrt{gH}$ and the height goes to $\frac{1}{2}$. There is clear convergence toward the analytical solution upon grid refinement, as is observed from Table 2.

We note that the pressure reported in Figure 11 is the pressure minus the exact interface pressure. The small difference from zero is, like in the shallow water example, attributed to the nonzero gas density. In order to obtain

TABLE 2
Convergence of $\overline{u}_{\text{out}}$ and h_{out} upon grid refinement

N	error in $\overline{u}_{\text{out}}$	error in h_{out}
50	0.030	0.0146
100	0.013	0.0064
200	0.004	0.0021

the current results, it was necessary to use formulation (51) with $p_{\text{int}} = 0$ in the first term on the right-hand side. This does not alter the solution in terms of liquid height or velocity, but circumvents numerical difficulties that can appear due to large pressure gradient close to the bubble nose in the original equations, which can lead to gas moving into the single-phase region.

5. CONCLUSIONS

In this paper, we have studied the simulation of elongated bubbles in channels, and more specifically the capability of the two-fluid model to compute the correct bubble drift velocity, which is the velocity of a bubble moving into a stagnant fluid.

We found that:

- The inviscid, incompressible solution by Benjamin [1] can be reproduced by solving the full incompressible Navier–Stokes equations with CFD, starting from the dam-break problem.
- The two-fluid model yields the same solution as the shallow water equations when applied to the dam-break problem. The bubble drift velocity obtained from the two-fluid model (or from the shallow water equations) is therefore $\sqrt{gH}$, instead of $\frac{1}{2}\sqrt{gH}$ as found in the Benjamin solution.
- The momentum equation of the two-fluid model misses two terms that are necessary to obtain the correct bubble drift velocity: the horizontal momentum correction parameter β and the variation of the pressure over the channel height due to vertical momentum flux. By computing these values from the Benjamin bubble solution, the correct bubble drift velocity can be obtained from the two-fluid model.

The main conclusion of this paper is, therefore, the two-fluid model in its standard form is not able to correctly reproduce the bubble drift velocity as predicted by the Benjamin bubble. A similar conclusion will hold for a pipe instead of a channel. To make the two-fluid usable for bubble simulations, such as in pipeline flushing, two adaptations are needed: an estimate of the momentum flux correction parameter β, and an estimate of the vertical momentum flux. In future work we will investigate how these can be determined based on reconstruction of velocity profiles. However, at the same time we realize that the extension to viscous flows has to be made. In viscous flows, the effect of the vertical momentum flux might be less substantial than in inviscid flow, and the major contribution in predicting the correct bubble drift velocity is expected to be the momentum correction parameter.

REFERENCES

[1] Benjamin, T.B. (1968) Gravity currents and related phenomena. *Journal of Fluid Mechanics.*, 31 (02): 209–248.

[2] Dumitrescu, D.T. (1943) Stromung an einer Luftblase im senkrechten Rohr. *ZAMM - Journal of Applied Mathematics and Mechanics/Zeitschrift für Angewandte Mathematik und Mechanik*, 23 (3): 139–149.

[3] Davies, R.M. and Taylor, G. (1950) The mechanics of large bubbles rising through extended liquids and through liquids in tubes. *Proceedings of the Royal Society of London. Series A. Mathematical and Physical Sciences.*, 200 (1062): 375–390.

[4] Nicklin, D.J., Wilkes, J.O. and Davidson, J.F. (1962) Two-phase flow in vertical tubes. *Trans. Inst. Chem. Eng.*, 40: 61–68.

[5] Stewart, B.H. and Wendroff, B. (1984) Two-phase flow: Models and methods. *Journal of Computational Physics*, 56 (3): 363–409.

[6] Ishii, M. and Hibiki, T. (2010) *Thermo-Fluid Dynamics of Two-Phase Flow*; Springer Verlag.

[7] Ishii, M. and Mishima, K. (1984) Two-fluid model and hydrodynamic constitutive relations. *Nuclear Engineering and Design*, 82 (23): 107–126.

[8] Song, J. and Ishii, M. (2001) The one-dimensional two-fluid model with momentum flux parameters. *Nuclear Engineering and Design*, 205 (12): 145–158.

[9] Montini, M. (2011) *Closure relations of the one-dimensional two-fluid model for the simulation of slug flows;* PhD thesis, Imperial College.

[10] Inácio, J.R.G., Carneiro, J.N.E., and Nieckele, A.O. (2012) Investigation of closure relations for 1D two-fluid model in vertical pipes. In *14th Brazilian Congress of Thermal Sciences and Engineering.*

[11] Andreussi, P., Bonizzi, M., and Vignali, A. (2009) Motion of elongated gas bubbles over a horizontal liquid layer. In *Proc. 14th Int. Conf. on Multiphase Production Technology, BHR.*

[12] Billingham, J. and King, A.C. (2000) *Wave motion*; Cambridge University Press.

[13] Kroes, R.F. and Henkes, R.A.W.M. (2014) CFD for the motion of elongated gas bubbles in viscous liquid. In *Proc. 9th American Conf. Multiphase Technology, BHR*, number 2014-E3, pages 283–298.

APPENDIX: DETAILS OF DISCRETIZATION OF TWO-FLUID MODEL

A.1 Spatial Discretization

We discretize the two-fluid model, equations (21)-(25), by using a FVM on a staggered grid. As indicated in Figure A.12, the staggered grid consists of both *p*-volumes, Ω^p, and *u*-volumes, Ω^u. Each volume consist of liquid and gas phase: $\Omega = \Omega_l \cup \Omega_g$, for both *u*- and *p*-volumes.

We start with conservation of mass for a phase α (α is liquid or gas), leaving out the explicit indication of averaging:

$$\frac{\partial}{\partial t}(\rho_\alpha h_\alpha) + \frac{\partial}{\partial x}(\rho_\alpha h_\alpha u_\alpha) = 0. \tag{52}$$

Integration of (52) over $(\Omega_\alpha^p)^i$ gives:

$$\frac{d}{dt}\left(\Omega_p^i \rho_\alpha^i\right) + (\rho_\alpha h_\alpha)^{i+1/2} u_\alpha^{i+1/2} - (\rho_\alpha h_\alpha)^{i-1/2} u^{i-1/2} = 0, \tag{53}$$

with the finite volume size approximated by

$$\Omega_p^i = h_\alpha^i \Delta x_p^i. \tag{54}$$

The finite volume size can be used to rewrite the semi-discrete equation for conservation of mass into:

$$\frac{d}{dt}\left(\rho_\alpha^i h_\alpha^i\right) + \frac{1}{\Delta x_p^i}\left((\rho_\alpha h_\alpha)^{i+1/2} u_\alpha^{i+1/2} - (\rho_\alpha h_\alpha)^{i-1/2} u_\alpha^{i-1/2}\right) = 0. \tag{55}$$

The term $(\rho_\alpha h_\alpha)^{i+1/2}$ requires interpolation from neighbouring values, which is described below. The equation for the conservation of momentum for phase α reads

$$\frac{\partial}{\partial t}(\rho_\alpha u_\alpha) + \frac{\partial}{\partial x}(\rho_\alpha h_\alpha u_\alpha^2) = -h_\alpha \frac{\partial p_{int}}{\partial x} - \frac{\partial}{\partial x}\left(\frac{1}{2}\rho_\alpha g h_\alpha^2\right), \tag{56}$$

Integration of (56) over $(\Omega_\alpha^u)^{i+1/2}$ gives:

$$\frac{d}{dt}\left(\Omega_u^{i+1/2} \rho_\alpha^{i+1/2} u_\alpha^{i+1/2}\right) + (\rho_\alpha h_\alpha)^{i+1}(u_\alpha^{i+1})^2 - (\rho_\alpha h_\alpha)^i (u_\alpha^i)^2 = -h_\alpha^{i+1/2}(p^{i+1} - p^i) - \left(\frac{1}{2}\rho_\alpha^{i+1} g(h_\alpha^{i+1})^2 - \frac{1}{2}\rho_\alpha^i g(h_\alpha^i)^2\right), \tag{57}$$

where

$$\Omega_u^{i+1/2} = h_\alpha^{i+1/2} \Delta x_u^{i+1/2}. \tag{58}$$

Several terms in (55) and (57) require approximation. All terms that are not part of the convective terms are interpolated using a central scheme, e.g., $h_\alpha^{i+1/2} = \frac{1}{2}(h_\alpha^i + h_\alpha^{i+1})$. The convective terms, on the other hand, require more care in order to prevent numerical oscillations. They are computed in an upwind fashion using a high resolution scheme as follows. Let ϕ denote a generic quantity on a cell face (either u^2 or ρh) and let θ be a smoothness indicator, given by

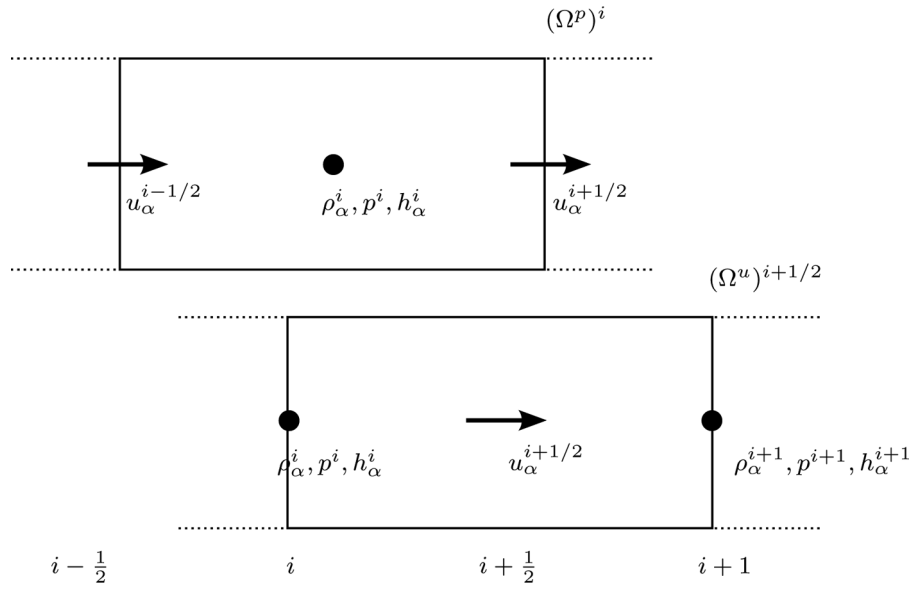$$\theta^{i+1/2} = \frac{\phi_c - \phi_u}{\phi_d - \phi_c}, \tag{59}$$

$(\Omega^p)^i$

$u_\alpha^{i-1/2}$ $\rho_\alpha^i, p^i, h_\alpha^i$ $u_\alpha^{i+1/2}$

$(\Omega^u)^{i+1/2}$

$\rho_\alpha^i, p^i, h_\alpha^i$ $u_\alpha^{i+1/2}$ $\rho_\alpha^{i+1}, p^{i+1}, h_\alpha^{i+1}$

$i - \frac{1}{2}$ $\qquad$ i $\qquad$ $i + \frac{1}{2}$ $\qquad$ $i+1$

FIG. A.12. Staggered grid layout.

where

$$\left.\begin{array}{ccc}\phi_u & = & \phi^{i-1}\\ \phi_c & = & \phi^i\\ \phi_d & = & \phi^{i+1}\end{array}\right\}\text{if } u^{i+1/2} \geq 0 \;, \quad \left.\begin{array}{ccc}\phi_u & = & \phi^{i+2}\\ \phi_c & = & \phi^{i+1}\\ \phi_d & = & \phi^i\end{array}\right\}\text{if } u^{i+1/2} < 0,$$

[60]

and ϕ_d, ϕ_u and ϕ_c denote the downstream, upstream and directly upstream quantities of the face under consideration. The smoothness indicator is used to compute a slope-limiter $l(\theta)$, from which the face quantity follows as:

$$\phi^{i+1/2} = \phi_c + \frac{1}{2}l^{i+1/2}(\phi_d - \phi_c).$$

[61]

In the current study the van Albada limiter,

$$l(\theta) = \frac{\theta^2 + \theta}{\theta^2 + 1},$$

[62]

has been used, mainly because of its continuous differentiability, which is a favourable property when the fully discrete equations are solved with a Newton solver.

A.2 Temporal Discretization

The semi-discrete equations (55) and (57) can be written in the form

$$\dot{U} = \mathbf{F}(\mathbf{U}),$$

[63]

where U is the vector of conserved variables

$$\boldsymbol{U} = \begin{bmatrix} (\rho_l h_l)_1, (\rho_l h_l)_2, \ldots, (\rho_g h_g)_1, \ldots, \\ (\rho_l h_l u_l)_1, \ldots, (\rho_g h_g u_g)_1, \ldots \end{bmatrix}^T.$$

[64]

The semi-discrete equations are solved with the BDF2 scheme:

$$\frac{\boldsymbol{U}^{n+1} - \frac{4}{3}\boldsymbol{U}^n + \frac{1}{3}\boldsymbol{U}^{n-1}}{\Delta t} = \frac{2}{3}\boldsymbol{F}(\boldsymbol{W}^{n+1}),$$

[65]

where we evaluate $\mathbf{F}$ in terms of the primitive variables W:

$$\boldsymbol{W} = \begin{bmatrix} (h_l)_1, \ldots, (u_l)_1, \ldots, (u_g)_1, \ldots, p_1, \ldots \end{bmatrix}^T.$$

[66]

Equation (65) forms a non-linear system of equations that is solved using a Newton approach:

$$\left[\frac{1}{\Delta t}\left(\frac{\partial \boldsymbol{U}}{\partial \boldsymbol{W}}\right)^m - \frac{2}{3}\left(\frac{\partial \boldsymbol{F}}{\partial \boldsymbol{W}}\right)^m\right]\Delta \boldsymbol{W} = $$
$$-\left[\frac{\boldsymbol{U}^m - \frac{4}{3}\boldsymbol{U}^n + \frac{1}{3}\boldsymbol{U}^{n-1}}{\Delta t} - \frac{2}{3}\boldsymbol{F}(\boldsymbol{W}^m)\right].$$

[67]

To solve the non-linear system, we solve for the increments in the primitive variables $\Delta\mathbf{W}$, but the final system that is solved is (65), and as a consequence mass and momentum will be conserved. The Jacobians $\frac{\partial U}{\partial W}$ and $\frac{\partial F}{\partial W}$ are computed automatically by using finite differences. The constraint in the form $h_g = H - h_l$ is used to close the system of equations.